

Methodological errors due to a non-cylindrical surface in a Jones-type cell with a removable central extension tube

Oleksandr Mikhal¹, Dmytro Meleshchuk¹, Oleksii Stennik²

¹ Institute of Electrodynamics of the National Academy of Sciences of Ukraine, 56 Peremohy Ave, Kyiv, 03057, Ukraine

² Ukrmetrteststandart, 4 Metrologichna St, Kyiv, 03143, Ukraine

ABSTRACT

The article shows an idealized model of a Jones-type cell with a removable central extension tube. Two main factors leading to the cylindrical distortion of the inner surface of the cell are considered. These are radial displacement and tube diameter inequality. Based on the finite element method (FEM), errors in measuring the resistance of a liquid column caused by the non-uniformity of the current density distribution inside the cell were determined. The methodological error with respect to the idealized model was estimated for each factor separately and in combination. The Authors show that at a radial displacement of 0.6 mm, the error can reach 0.1 %. The same error value occurs when the inequality of the diameters is only 20 μm .

Section: RESEARCH PAPER

Keywords: Electrolytic conductivity; Measurement error; Jones-type cell; Radial displacement; Finite element analysis

Citation: Oleksandr Mikhal, Dmytro Meleshchuk, Oleksii Stennik, Methodological errors due to a non-cylindrical surface in a Jones-type cell with a removable central extension tube, Acta IMEKO, vol. 12, no. 4, article 24, December 2023, identifier: IMEKO-ACTA-12 (2023)-04-24

Section Editor: Laura Fabbiano, Politecnico di Bari, Italy

Received July 4, 2023; **In final form** November 14, 2023; **Published** December 2023

Copyright: This is an open-access article distributed under the terms of the Creative Commons Attribution 3.0 License, which permits unrestricted use, distribution, and reproduction in any medium, provided the original author and source are credited.

Corresponding author: Oleksii Stennik, e-mail: metrology@protonmail.com

1. INTRODUCTION

According to the international standard [1], the electrolytic conductivity (EC) k ($\text{S}\cdot\text{m}^{-1}$) is defined as the quotient of the magnitude of electric current density J ($\text{A}\cdot\text{m}^{-2}$) and the magnitude of electric field strength E ($\text{V}\cdot\text{m}^{-1}$) [2]. In the system of fundamental physical quantities, EC has the following dimension:

$$\dim k = \frac{T^3 I^2}{M L^3} \quad (1)$$

This expression reflects the connection of EC with the measurement standards of mass M (kg), length L (m), time T (s), and electric current I (A). However, in practice, it is extremely inconvenient to use the above quantities as well as the electric current density and electric field strength. For these reasons, at present, for the practical realization of the EC unit, conductivity cells with a well-defined geometry are used. The dimensions of such cells are accurately measured. The main types of such primary cell designs are a Jones-type cell with a removable central extension tube [3]-[7] and a cell with a movable electrode [6]-[10].

Both types of cell designs implement the differential method of measurement. The main purpose of using the differential

method is to suppress the effect of electrochemical impedance on the electrode/electrolyte interfaces [11]-[17]. The measurement result using the differential method is the resistance of the “virtual” liquid column, which is formed as a consequence of the difference in the lengths of the two liquid columns.

Jones-type cells with a removable central extension tube have become widespread among national metrological institutes (NMIs) for the practical realization of the EC unit. This design was first proposed and developed at the National Institute of Standards and Technology (NIST, Gaithersburg) more than 30 years ago [18]. However, even at the present stage, such a principle is used in the establishment of national measurement standards, for example, at the National Metrology Institute of Japan (NMIJ) [5]. The central extension tube of such a cell can be removed in order to shorten the distance between the electrodes, thereby reducing the liquid column resistance, or it may be put back, thereby increasing the resistance.

However, this method is based on the assumption that the lines of current density J ($\text{A}\cdot\text{m}^{-2}$) inside the cell are not distorted after assembling. But in fact, the inner surface of a conductivity cell of this design can have a stepped shape. This can be caused by existing radial displacements between the axes of the tubes or

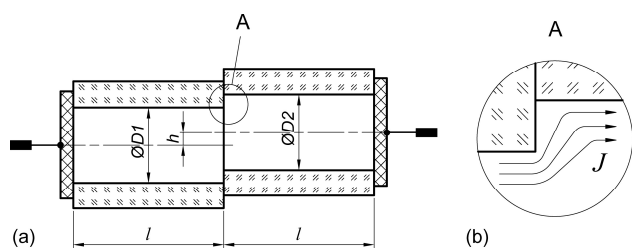


Figure 1. Simplified physical model of a Jones-type cell without a central extension tube when the radial displacement occurs.

by diameter inequality. These phenomena are equivalent to a change in the effective cross-sectional area of the liquid column and lead to errors in the measurement of resistance.

The purpose of this article is to develop mathematical models of liquid columns and obtain quantitative characteristics of the errors that may occur when measuring the resistance of a cell of this design. In order to simulate the current density distribution inside the cell and the electrical resistance of the electrolyte columns, the finite element method (FEM) was used [19]. This method is widely used and is not new in electrochemistry. It is often used to test the electric field uniformity when designing conductivity cells [5] or even when modeling the electrochemical impedance and capacitance of electrode systems [20].

2. PHYSICAL AND MATHEMATICAL MODELS

2.1. Physical model of a cell

The cell with a removable central extension tube consists of three sections. The first two are secondary Jones-type cells [4], [21], [22] cut in half. Each of the half-cells has a length of l (m). A simplified physical model of the cell, which will later be used to calculate the resistance without a central extension tube, is shown in Figure 1(a). It has one joint where radial displacement can occur, denoted as h (m). This displacement makes the outer surface of the liquid column stepped. Correspondingly, the lines of current density J ($A \cdot m^{-2}$) inside the cell are distorted; see Figure 1(b).

The third section of the cell is a removable extension tube of length L (m), inserted between two half-cells. Simplified physical models of a cell of three tubes are shown in Figure 2. The cell with the removable central tube has two joints with the side tubes. Accordingly, the radial displacement can only be at one joint, and there is no displacement at the other (see Figure 2(a)). Radial displacement can occur at two joints. In this case, the radial displacements at the joints can be in opposite directions relative to the central tube (with different signs) (see Figure 2(b)), or they can be in one direction (with one sign) (see Figure 2(c)).

The operation algorithm is as follows: First, the resistance R_{m1} (Ω) is measured with a liquid column length of $2l$ (without a central extension tube). Then the length of the liquid column is increased to $2l + L$ by putting the central extension tube between two half-cells, and resistance R_{m2} (Ω) is measured. The EC is expressed by the equation [8]-[10]:

$$k = \frac{L}{A} \frac{1}{R_{m2} - R_{m1}} = \frac{4L}{\pi D^2} \frac{1}{R_{m2} - R_{m1}}, \quad (2)$$

where L (m) is a “virtual” liquid column length, A (m^2) is the cross-sectional area of a cell, and D (m) is the inner diameter of the cell. This basic equation is used to determine the EC in almost all national measurement standards with a two-electrode primary cell.

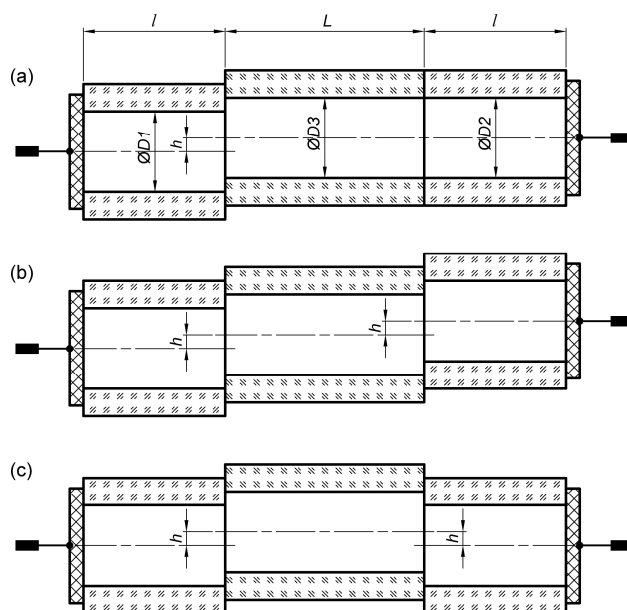


Figure 2. Simplified physical models of a Jones-type cell with a central removable extension tube when the radial displacement occurs.

The problem is that equation (2) is valid only under the condition of a uniform distribution of field lines inside the cell. The equation is based on the following axiom. The resistance of the liquid column is determined only by the EC of the solution k ($S \cdot m^{-1}$) and the geometrical dimensions of the liquid column, length L (m), and cross-sectional area A (m^2) [3], [22]:

$$R_{\text{hom}} = \frac{L}{A} \frac{1}{k} = \frac{4L}{\pi D^2} \frac{1}{k}. \quad (3)$$

In turn, the idealized model (2) was obtained with an ideal outer surface of the electrolyte column in the form of a straight circular cylinder. However, in general terms, at least two factors leading to a stepped surface of the electrolyte column can be identified. The first factor is the tube diameter inequality. The difference in diameters is determined by the manufacturing technology. It will be minimal when all three tubes are made from the same workpiece. The second factor is determined by the radial displacement that can occur during permanent central tube removals. Each of these factors leads to the fact that the measurement result will not correspond to the idealized model - the resistance of a liquid column with a uniform field inside. As a result, there is a relative error δ_R (%) when measuring the resistance of the liquid column:

$$\delta_R = \frac{R_{m,i} - R_{\text{hom},i}}{R_{\text{hom},i}} \cdot 100, \quad (4)$$

where $R_{m,i}$ (Ω) is the measurement result (resistance of the liquid column under conditions of a non-uniform field), and $R_{\text{hom},i}$ (Ω) is the resistance of the liquid column under conditions of a homogeneous field (idealized model).

2.2. Mathematical model of a cell

In order to calculate the resistance $R_{m,i}$ (Ω) and, accordingly, the error (4), a mathematical model was used. It is based on a field theory in which the distribution of the scalar electric potential corresponds to the three-dimensional Laplace's equation [16], [17] in rectangular Cartesian coordinates:

$$\frac{\partial^2 E}{\partial x^2} + \frac{\partial^2 E}{\partial y^2} + \frac{\partial^2 E}{\partial z^2} = 0. \quad (5)$$

Calculation of the resistance of the liquid column $R_{m,i}$ (Ω) was carried out according to equation (6), where the measuring voltage U_{cell} (V) was set as a constant and the electric current through the cell I_{cell} (A) was calculated by integrating the z -component of the electric current density J_z ($\text{A}\cdot\text{m}^{-2}$) over the cross-sectional area A (m^2) [23]:

$$R_{m,i} = \frac{U_{\text{cell}}}{I_{\text{cell}}} = \frac{U_{\text{cell}}}{\int_A J_z \, dA}. \quad (6)$$

Equations (5), (6) are standard built-in functions of many software products designed for modelling various physical phenomena by the finite element method. In this study, so as to estimate the resistance of the cell filled with the solution and obtain quantitative characteristics for a range of geometrical parameters of the cell, Comsol Multiphysics® software was used.

When modelling, the following parameters were set: EC of the solution: $k = 0.1 \text{ S}\cdot\text{m}^{-1}$, voltage on the electrodes of the cell: $U_{\text{cell}} = 1 \text{ V}$, relative permittivity of the solution: $\epsilon_r = 77$ [24], the boundaries of the model are electrically isolated, and the result of solving the model is the resistance between the electrodes.

The accuracy of the simulation result is greatly influenced by the size of the mesh elements of the 3D model. This is especially critical for small models with high surface curvature. The following parameters for the size of tetrahedral mesh elements were used in the simulation: maximum element size: $2.2\cdot 10^{-3} \text{ m}$, minimum element size: $2.2\cdot 10^{-5} \text{ m}$, maximum element growth rate: 1.3, curvature factor: 0.2, resolution of narrow regions: 1. These settings correspond to the predefined setting “extremely fine”. A typical mesh of a liquid column 3D model is shown in Figure 3.

3. SIMULATION RESULTS

As an object for specific calculations, a conductivity cell with the following dimensions was chosen: $D = 20 \text{ mm}$, $l = 40 \text{ mm}$, $L = 60 \text{ mm}$. These geometrical parameters are very close to the primary cell dimensions used in the Slovak and Japanese NMIs [6], [5]. In this study, error (4) was calculated, considering three possible variants of cylindricity distortion of the liquid column surface.

3.1. Option 1

There are two tubes with the same inner diameter: $D_1 = D_2 = D$. Nevertheless, with each assembling of the cell, radial displacements h (m) can occur. Only one displacement is possible when measuring the resistance R_{m1} (Ω) to calculate the EC (2). A physical model of such a cell is shown in Figure 1(a).

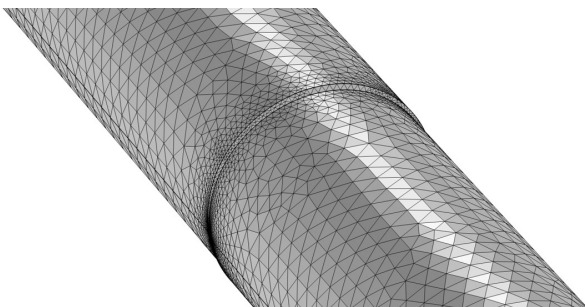


Figure 3. A typical mesh of a liquid column model with a radial displacement.

The error (4) that may occur in this case and is expressed by equations (3)-(6) is shown in Figure 4(a) and Figure 4(b).

Two displacements are possible when measuring the resistance R_{m2} to calculate the EC (2). Their physical models are shown in Figure 2. The error that may occur in this case and is expressed by equations (3)-(6) is shown in Figure 5. The error plots for the model in Figure 2(b) and 2(c) are the same. This means that the non-uniform fields due to each displacement do not overlap. Accordingly, the error due to two displacements does not depend on their relative positions. However, this error depends on the number of displacements. According to the results, the errors are additively combined.

3.2. Option 2

In order to simplify the computational procedures, only the model in Figure 1 was considered. The following conditions were set: there is no radial displacement $b = 0$, but nevertheless, due to technological defects in the manufacture of tubes, they have different diameters $D_1 \neq D_2$. The difference in diameters is denoted as follows: $D_1 - D_2 = \Delta D$. Error (4) due to the possible difference in diameters ΔD (μm) was calculated for two values of the inner diameter $D = 10 \text{ mm}$ and $D = 20 \text{ mm}$. The results are shown in Figure 6(a). If one compares these results with the plots in Figure 4(a), it is obvious that for $D = 20 \text{ mm}$, the difference in diameters causes a 30 times greater error than the radial displacement.

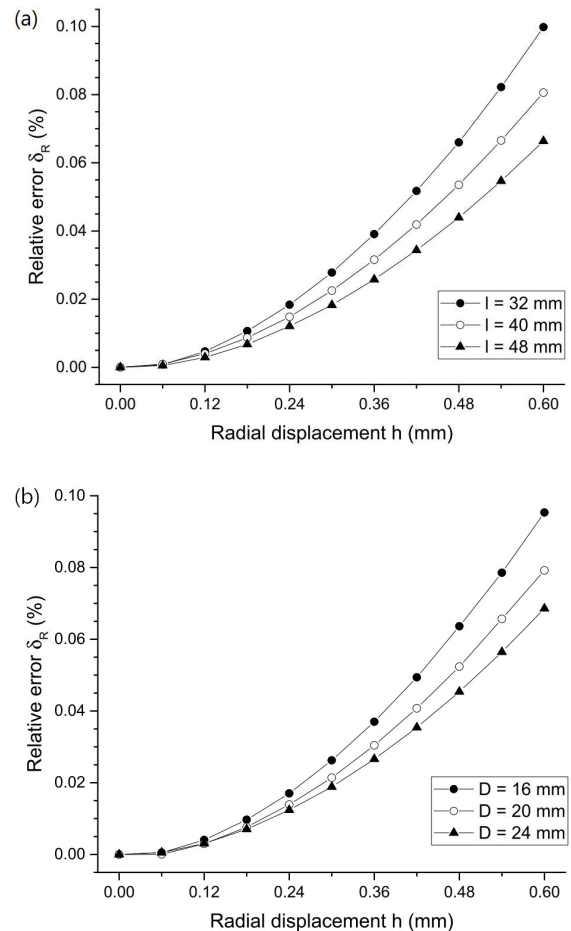


Figure 4. Dependencies of the resistance bias δ_R (%) on the radial displacement h (mm):

- (a): assembly of 2 tubes, $D_1 = D_2 = 20 \text{ mm}$, $l = 32 \text{ mm}/40 \text{ mm}/48 \text{ mm}$.
(b): assembly of 2 tubes, $l = 40 \text{ mm}$, $D = 16 \text{ mm}/20 \text{ mm}/24 \text{ mm}$.

3.3. Option 3

The third option is a combination of the first two. Also, in order to simplify the computational procedures, only the model in Figure 1 was considered. Error (4) is calculated under the condition that there is a radial displacement $h \neq 0$ and a difference in diameters $D_1 - D_2 = \Delta D$. The results of calculating the error as a function of the possible radial displacement h (m) for three values of the difference in the inner diameters of tubes ΔD (μm) are shown in Figure 6(b).

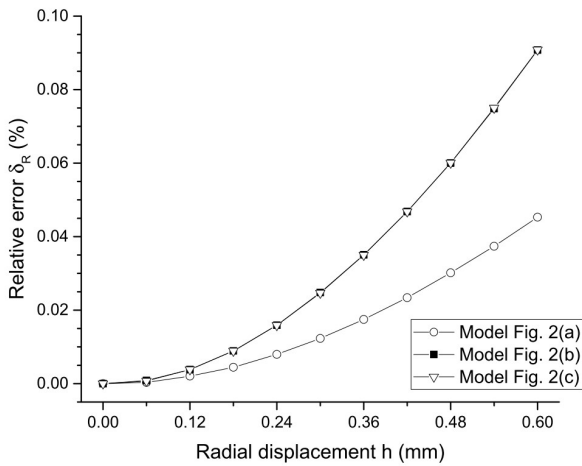


Figure 5. Dependencies of the resistance bias δ_R (%) on radial displacement h (mm). Assembly of 3 tubes, $D = 20$ mm, $l = 40$ mm, $L = 60$ mm.

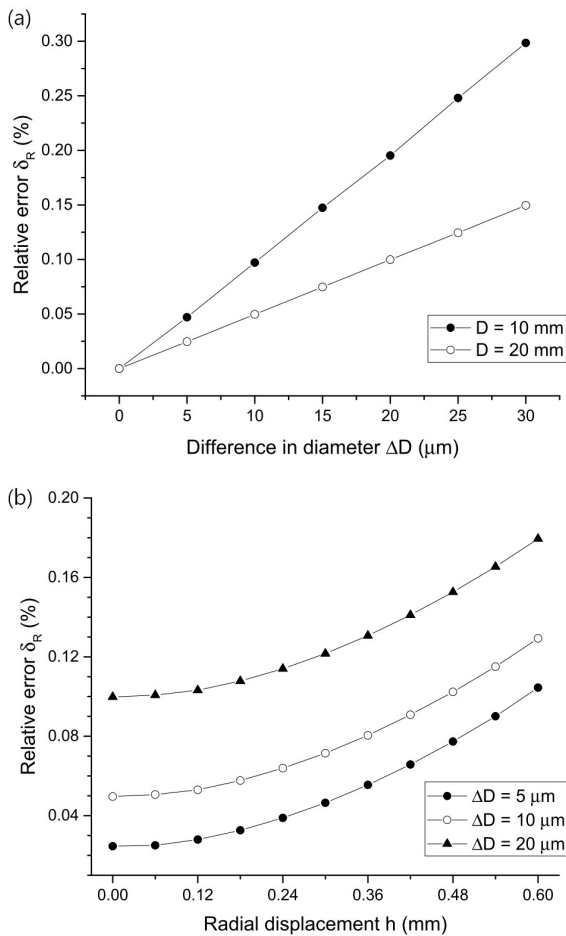


Figure 6. Dependencies of the resistance bias δ_R (%) on the difference in diameter ΔD (μm) and radial displacement h (mm). (a): assembly of 2 tubes, $l = 40$ mm, $h = 0$, $D_1 \neq D_2 \approx 10$ mm/20 mm. (b): assembly of 2 tubes, $l = 40$ mm, $h \neq 0$, $D_1 \neq D_2 \approx 20$ mm, $\Delta D = 5$ $\mu\text{m}/10$ $\mu\text{m}/20$ μm .

4. ACCURACY OF THE RESULTS

In order to evaluate the accuracy of the results of modelling by the finite element method, the resistance value R_s (Ω) obtained by solving the 3D models of cylindrical liquid columns was compared to the resistance R_{hom} (Ω) calculated from the geometrical dimensions of the ideal model using equation (3). The error of the simulation results δ_s (%) was determined by the following:

$$\delta_s = \frac{R_s - R_{\text{hom}}}{R_{\text{hom}}} \cdot 100. \quad (7)$$

The results for small models are especially informative since they have the highest surface curvature. The results of calculating the error δ_s (%) (7) for some models are given in Table 1. In all cases of solving the models that were carried out, the error δ_s (%) (7) did not exceed 0.0002 %.

5. DISCUSSION

The formation of a stepped liquid column when using a differential Jones-type cell leads to a significant distortion of the current density distribution (see Figure 7) and, as a result, to an error in measuring the resistance δ_R (%) (4).

The error shown in Figure 6(a) is deterministic. Therefore, it can be used to reduce the systematic error. Regarding the errors in Figure 4(a), Figure 4(b), Figure 5, and Figure 6(b), it should be noted that the displacement h (m) is difficult to control in the measurement. Its magnitude is not known in advance. Therefore, these errors should be attributed to random errors. The probability density function of such an error is also unknown in advance. By intuition, it should be Gaussian, but we cannot prove it. However, if the cell design allows the maximum possible radial displacement to be determined, the type B uncertainty caused by the radial displacement can be estimated using a rectangular distribution function.

Table 1. Accuracy of simulation results.

Geometrical dimensions of a liquid column	Calculated value R_{hom} (Ω)	Simulation result value R_s (Ω)	Simulation result error δ_s (%)
$D = 1$ mm, $L = 100$ mm	1,273,239.54	1,273,242.04	0.00020
$D = 9$ mm, $L = 40$ mm	6,287.60269	6,287.61038	0.00012
$D = 10$ mm, $L = 10$ mm	1,273.23954	1,273.23975	0.000016
$D = 25$ mm, $L = 100$ mm	2,037.18327	2,037.18507	0.000088

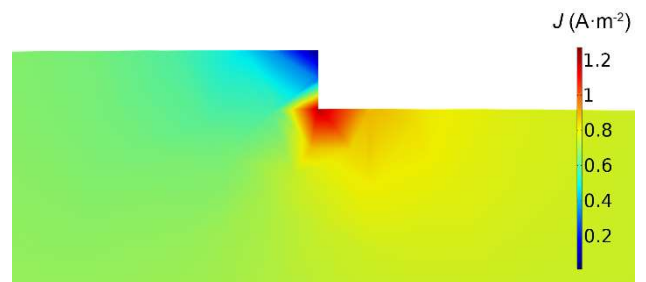


Figure 7. Current density distribution J ($\text{A} \cdot \text{m}^{-2}$) in the central slice of the liquid column model with a radial displacement ($D = 20$ mm, $l = 40$ mm, $L = 60$ mm, $h = 0.6$ mm).

6. CONCLUSIONS

1. Resistance measurements of primary conductivity cells of several national measurement standards [3]–[6] can be accompanied by an error of 0.08 % when the tubes are displaced without a central tube by 0.6 mm. When measuring resistance with a central tube under conditions of two displacements, the error can reach 0.1 %. Since the value of the displacement is not known in advance, these errors are considered random. They cannot be used as corrections to reduce the systematic error but must be taken into account when calculating the expanded uncertainty during international comparisons.

2. When measuring the resistance of a cell with a central tube, field non-uniformities due to each displacement do not overlap. They do not depend on the relative positions of the two displacements. This is explained by the fact that for the typical tube dimensions chosen for the study, the response to a jump in the field strength, when the ideal cylindricality of the surface is distorted, has time to level off before the next displacement.

3. The diameter difference causes a significantly larger error than the radial displacement. However, this type of error can be used to reduce the systematic error.

ACKNOWLEDGEMENT

The Authors would like to thank Leoš Vyskočil of the National Metrology Institute of Slovakia (SMU) for the idea of assessing the error due to radial displacement and for providing information on the primary conductivity cell geometry.

REFERENCES

- [1] ISO 80000-9:2019 Quantities and units - Part 9: Physical chemistry and molecular physics.
- [2] IEC 80000-6:2022 Quantities and units - Part 6: Electromagnetism.
- [3] R. H. Shreiner, K. W. Pratt, Standard reference materials: Primary standards and standard reference materials for electrolytic conductivity, in: NIST Special Publication 260-142., 2004 Ed. U.S. Government Printing Office, Washington, 2004.
- [4] C. Thirstrup, L. Deleebeeck, Review on electrolytic conductivity sensors, IEEE Trans. Instrum. Meas. 70 (2021), pp. 1–22. DOI: <https://doi.org/10.1109/TIM.2021.3083562>
- [5] T. Asakai, I. Maksimov, S. Onuma, T. Suzuki, T. Miura, A. Hioki, New Japanese certified reference materials for electrolytic conductivity measurements, Accreditation Qual. Assur. 22 (2017), pp. 73–81. DOI: [10.1007/s00769-017-1253-0](https://doi.org/10.1007/s00769-017-1253-0)
- [6] F. Brinkmann, N. E. Dam, E. Deák, F. Durbiano, E. Ferrara, J. Fűkő, H. D. Jensen, M. Máriássy, (+ 5 more authors), Primary methods for the measurement of electrolytic conductivity, Accreditation Qual. Assur. 8 (2003), pp. 346–353. DOI: [10.1007/s00769-003-0645-5](https://doi.org/10.1007/s00769-003-0645-5)
- [7] P. Spitzer, S. Seitz, Electrolytic conductivity, in: Handbook of metrology and testing, H. Czichos, T. Saito, L. Smith. Springer, Heidelberg, 2011, ISBN: 978-3-642-16640-2, pp. 498–507.
- [8] I. C. S. Fraga, P. P. Borges, B. S. R. Marques, W. B. S. Junior, S. P. Sobral (+ 4 more authors), Primary Measurements of Electrolytic Conductivity in Brazil, Proc. of Simposio de Metrología 2008, Santiago de Querétaro, México, 22–24 October 2008.
- [9] I. C. S. Fraga, J. C. Lopes, L. R. Cordeiro, L. F. Silva, P. P. Borges, Evaluation of the stability of solutions of low electrolytic conductivity by primary measurements, J. Solution Chem. 44 (2015), pp. 1920–1936. DOI: [10.1007/s10953-015-0384-3](https://doi.org/10.1007/s10953-015-0384-3)
- [10] K. C. Cunha, L. S. Pardellas, F. B. Gonzaga, Stability monitoring of electrolytic conductivity reference materials under repeated use conditions by the primary measurement method, J. Solution Chem. 49 (2020), pp. 306–315. DOI: [10.1007/s10953-020-00961-9](https://doi.org/10.1007/s10953-020-00961-9)
- [11] H. Sanabria, J. H. Miller, Relaxation processes due to the electrode-electrolyte interface in ionic solutions, Phys. Rev. E 74 (2006), pp. 051505–051505. DOI: [10.1103/PhysRevE.74.051505](https://doi.org/10.1103/PhysRevE.74.051505)
- [12] L. Pilon, H. Wang, A. d'Entremont, Recent advances in continuum modeling of interfacial and transport phenomena in electric double layer capacitors, J. Electrochem. Soc. 162 (2015), pp. A5158–A5178. DOI: [10.1149/2.0211505jes](https://doi.org/10.1149/2.0211505jes)
- [13] M. Becchi, L. Callegaro, F. Durbiano, V. D'Elia, A. Strigazzi, Novel impedance cell for low conductive liquids: Determination of bulk and interface contributions, Rev. Sci. Instrum. 78 (2007), pp. 113902–113902. DOI: [10.1063/1.2805195](https://doi.org/10.1063/1.2805195)
- [14] L. F. Lima, A. L. Vieira, H. Mukai, C. M. G. Andrade, P. R. G. Fernandes, Electric impedance of aqueous KCl and NaCl solutions: Salt concentration dependence on components of the equivalent electric circuit, J. Mol. Liq. 241 (2017), pp. 530–539. DOI: [10.1016/j.jmolliq.2017.06.069](https://doi.org/10.1016/j.jmolliq.2017.06.069)
- [15] O. Bottauscio, P. P. Capra, F. Durbiano, A. Manzin, Modeling of cells for electrolytic conductivity measurements, IEEE Trans. Magn. 42 (2006), pp. 1423–1426. DOI: [10.1109/TMAG.2006.871443](https://doi.org/10.1109/TMAG.2006.871443)
- [16] S. Seitz, A. Manzin, H. D. Jensen, P. T. Jakobsen, P. Spitzer, Traceability of electrolytic conductivity measurements to the International System of Units in the sub mSm⁻¹ region and review of models of electrolytic conductivity cells, Electrochim. Acta 55 (2010), pp. 6323–6331. DOI: [10.1016/j.electacta.2010.06.008](https://doi.org/10.1016/j.electacta.2010.06.008)
- [17] A. Manzin, O. Bottauscio, D. P. Ansalone, Application of the thin-shell formulation to the numerical modeling of Stern layer in biomolecular electrostatics, J. Comput. Chem. 32 (2011), pp. 3105–3113. DOI: [10.1002/jcc.21896](https://doi.org/10.1002/jcc.21896)
- [18] Y. C. Wu, K. W. Pratt, W. F. Koch, Determination of the absolute specific conductance of primary standard KCl solutions, J. Solution Chem. 18 (1989), pp. 515–528. DOI: [10.1007/BF00664234](https://doi.org/10.1007/BF00664234)
- [19] D. W. Pepper, J. C. Heinrich, The finite element method: Basic concepts and applications with MATLAB, MAPLE, and COMSOL, Third Edition. Taylor & Francis Group, Boca Raton, 2017, ISBN-13: 978-1-4987-3860-6, 628 pp. DOI: [10.1201/9781315395104](https://doi.org/10.1201/9781315395104)
- [20] S. Smith, How to Model Electrochemical Resistance and Capacitance. Online [Accessed 6 November 2023] <https://www.comsol.de/blogs/how-to-model-electrochemical-resistance-and-capacitance/>
- [21] F. S. H. Krismastuti, S. Sujarwo, A. Hindayani, N. Hamim, N. Tangpaisarnkul, W. Hongthani, Competency evaluation on electrolytic conductivity measurement in Indonesia by an unofficial bilateral comparison between RCChem-LIPI and NIMT, Accreditation Qual. Assur. 24 (2019), pp. 119–125. DOI: [10.1007/s00769-018-1360-6](https://doi.org/10.1007/s00769-018-1360-6)
- [22] Y. Hibino, T. Asakai, T. Suzuki, M. Ohata, Applicable measuring range of two-electrode type commercial electrolytic conductivity meter for accurate determination of electrolytic conductivity, J. Chem. 2022 (2022), pp. 9913667–9913667. DOI: [10.1155/2022/9913667](https://doi.org/10.1155/2022/9913667)
- [23] E. M. Purcell, D. J. Morin, Electricity and magnetism, Third Edition. Cambridge University Press, Harvard University, Massachusetts, 2013, ISBN 978-1-107-01402-2, pp. 177–186.
- [24] T. Chen, G. Hefter, R. Buchner, Dielectric Spectroscopy of Aqueous Solutions of KCl and CsCl, J. Phys. Chem. A 107 (2003), pp. 4025–4031. DOI: [10.1021/jp026429p](https://doi.org/10.1021/jp026429p)